Available online at www.sciencedirect.com
SCIENCE DIRECT
Journal of Power Sources 155 (2006) 118–127
JOURNAL OF POWER SOURCES
www.elsevier.com/locate/jpowsour

Methanol electrooxidation on Pt particles dispersed into PANI/SWNT composite films

Gang Wu *, Li Li, Jing-Hong Li, Bo-Qing Xu *

Innovative Catalysis Program, Key Laboratory of Organic Optoelectronics and Molecular Engineering, Department of Chemistry, Tsinghua University, Beijing 100084, China

Received 29 January 2005; received in revised form 22 April 2005; accepted 25 April 2005
Available online 29 June 2005

Abstract

Conducting polymer composite films comprised of polyaniline (PANI) and single wall carbon nanotubes (SWNT) was prepared by electrochemical codeposition during the electropolymerization in an aniline solution with suspending SWNT. The fabricated composite films are assessed with respect to their potential application as support materials in Pt electrocatalyst for electrochemical oxidation of methanol. The PANI/SWNT composite film incorporated with SWNT has a higher polymeric degree and lower defect density in PANI structure than PANI film. Furthermore, the incorporation of SWNT also leads to higher electrochemically accessible surface areas (S_a), electronic conductivity and easier charge-transfer at polymer/electrolyte interfaces, which make higher dispersion and utilization for deposited Pt. Therefore, the Pt particles electrodeposited on PANI/SWNT composite polymer film exhibits excellent catalytic activity and stability for the electrooxidation of methanol in comparison to Pt supported on PANI film, which reveals that the composite film is more promising for application in electrocatalyst as a support material.

Keywords: Polyaniline; SWNT; Composite support; Methanol electrooxidation; Pt particles

1. Introduction

Recently, there has been an increasing interest in the development of direct methanol fuel cells (DMFCs). However, the major problems of electrocatalyst in DMFC are the high loading of Pt and deactivation of Pt electrocatalyst [1,2]. It has been proved that the support materials in electrocatalysts play an important role to the electrochemical performance [3]. Though improvement has been made in the catalytic activity and stability of the electrocatalyst by effectively dispersing Pt and Pt based particles onto the various electronically conducting supports, much efforts is still continuing making. Besides traditional carbon support materials (XC-72), the appearance of novel carbon materials, such as graphite nanofibers (GNFs) [4,5], carbon nanotubes (CNTs) [6–8] and mesocarbon microbeads (MCMB) [9,10] provide new candidates of carbon supports for Pt and Pt based electrocatalyst.

On the other hand, to date, some new attempts have been made to design and synthesize conducting polymer/carbon nanotube composite materials for various target applications such as electrochemical devices, light-emitting diodes, chromatography, electrostatic discharge protection and corrosion-protecting paint [11–13]. Among them, composite made from single-walled carbon nanotubes (SWNT) and polyaniline (PANI) were synthesized through chemical routes used as printable conductors for organic electronic devices [14]. Here, we consider that the combination of PANI with SWNT would offer an attractive composite support material for electrocatalyst in DMFCs to enhance its activity and stability based on morphological modification or electronic interaction between two components. In this composite structure, the reason to chose polyaniline (PANI) as the polymer matrix from various conducing polymer, is due to its relatively wide potential stability (0–1.0 V) [15], reproducible synthesis

* Corresponding authors. Tel.: +86 10 62795834; fax: +86 10 62792122.
E-mail addresses: wugang@tsinghua.edu.cn (G. Wu), bqxu@tsinghua.edu.cn (B.-Q. Xu).

0378-7753/$ – see front matter © 2005 Elsevier B.V. All rights reserved.
doi:10.1016/j.jpowsour.2005.04.035

and good electronically conducting (1 to 10^2 S cm^{-1}) [16]. Meanwhile, SWNT exhibit high external surface, good electronic conductivity, low density, high mechanical strength and high stability. Therefore, the formation of hybrid materials by incorporation of SWNT into PANI matrix for the fabrication of PANI/SWNT composite support is an interesting approach to improve the properties of electrocatalyst materials because composite structure may exhibit improved characteristics with respect to the individual component compounds.

However, the low solubility of SWNT in most solvent limits the feasibility of synthesizing this kind composite film by chemical route [17]. To the best of our knowledge, there have been no reports either on the synthesis PANI/SWNT composite film by electrochemical codeposition or its use for support materials in the electrocatalytic oxidation of methanol. In this work, we describe the synthesis and characterization of PANI/SWNT composite film incorporated SWNT into PANI matrix via electrochemical composite codeposition technique during the process of electropolymerization. The PANI/SWNT composite film dispersed Pt by electrodeposition technique shows much higher mass activity and stability for methanol oxidation than a pure PANI film and is more promising for application in electrocatalyst.

2. Experimental

2.1. Preparation Pt-PANI/SWNT composite films

Single wall carbon nanotubes (SWNTs) employed in this work were provided by Nankai University and produced via CVD method [18]. A general method to purify and modify the nanotubes surface is a pretreatment by refluxing in $HCl + HNO_3$ solution (3:1) for 8 h, followed by an extensive washing with deionized water. After then, the pretreated SWNTs were suspended in a solution of 0.1 M $C_6H_5NH_2$ + 0.5 M H_2SO_4 with a concentration of 1 g L^{-1}. In addition, an ultrasonic generator was used to minimize the agglomeration of SWNTs before electropolymerization process. To electropolymerize PANI/SWNT, glassy carbon (GC) rotating disc electrode, as working electrode was carried out in the cycling potential range of 0.05–1.1 V at a sweep rate 50 mV s^{-1} using EG&G PAR 273 potentiostat–galvanostat. The thickness of PANI/SWNT films obtained was determined by the total anodic charge, supposing that charge of 16 mC cm^{-2} corresponds to a thickness of 0.063 μm [19]. To disperse Pt particles into polymer matrix, electrodeposition was conducted in 0.5 M H_2SO_4 containing 3 mM H_2PtCl_6 at constant potential 0.05 V for different time to obtain various Pt loadings. In order to deposit Pt particles uniformly, prior to the electrodeposition, the PANI/SWNT film were soaked in electrolytes for 15 min to let metal ions fully adsorb into PANI/SWNT films. After the electrodeposition, the H_2PtCl_6 electrolyte was replaced by the 0.5 M H_2SO_4 solution and potential sweeps between 0 and 0.95 V was continued until no change of anodic current. The purpose of these additional procedures is the elimination of traces of the Cl^-, which would poison the Pt catalysts.

2.2. Physical and electrochemical characterizations

The PANI and PANI/SWNT films were characterized by XPS using an ESCA 210 and MICROLAB 310D spectrometer. For recording the spectra Mg Kα ($h\nu$ = 1253.6 eV) irradiation was employed as the photon source with primary tension of 12 kV and emission current of 20 mA.

The observations of the morphology of PANI and PANI/SWNT before and after the electrodeposition Pt were carried out using a JEM-100S transmission electron microscope (TEM). In addition, Pt-PANI and Pt-PANI/SWNT samples were also performed on Hitachi S-5400 scanning electron microscopy (SEM) at 15 kV to determine the metal dispersion.

The glassy carbon RDE deposited PANI and PANI/SWNT films after 30 cycle electropolymerization were characterized as a working electrode in 0.5 M H_2SO_4 by cyclic voltammograms (CV) and electrochemical impedance spectroscopy (EIS) using an EG&G model 273 potentiostat/galvanostat and 1025 Frequency Response Detector. The sweep rate in CV measurement is 20 mV s^{-1}. EIS measurements were performed under open circuit potential between 100 kHz and 0.1 Hz frequency ranges with an excitation signal of 5 mV. To evaluate their impedance parameters, Zsimpwin fitting program was chosen to analyze the impedance spectra.

2.3. Methanol electrooxidation on Pt-PANI/SWNT

Methanol electrooxidation on the Pt-PANI and Pt-PANI/SWNT was examined by CV at 20 mV s^{-1} ranged from 0 to 0.95 V and current–time curves at 0.65 V in 0.5 M CH_3OH + 0.5 M H_2SO_4 solution. All the electrochemical experiments were carried out at 25 °C.

3. Results and discussion

3.1. Electropolymerization of PANI and PANI/SWNT films

To determine the effect of incorporated SWNT on polymer growth process, cyclic voltammograms (CV) for PANI and PANI/SWNT composite film during the electropolymerization at 1st, 20th and 30th cycle were shown in Fig. 1, respectively. During the electropolymerization process, an increase in the redox currents and an appearance of a greenish color characteristic of polyaniline emeraldine salt in solution around the electrodes are observable suggesting a growth of the polyaniline film. Moreover, there are three pairs of redox peaks labeled as A/A′–C/C′. The first redox peak at about

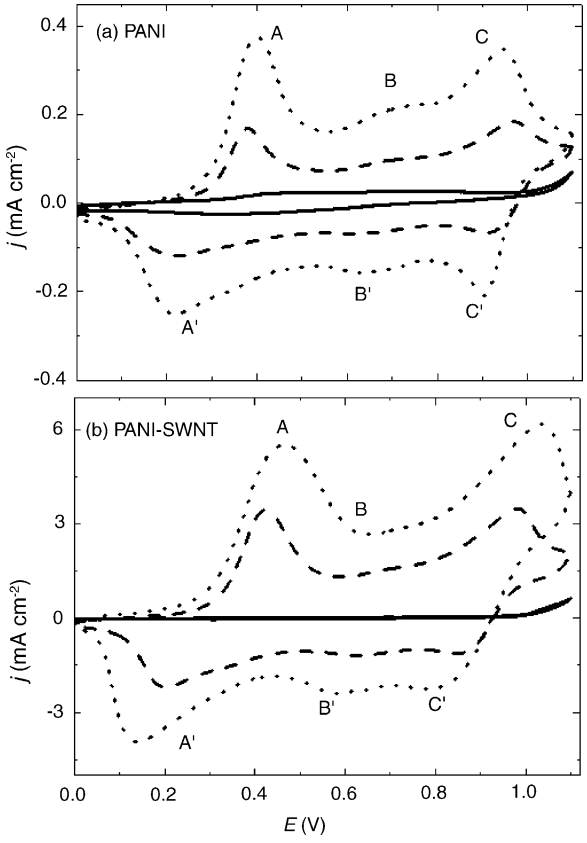

Fig. 1. Electropolymerization process of PANI (a) and PANI/SWNT (b) at 1st (—), 20th (– – –) and 30th (· · ·).

0.42 V corresponds to the transition of the polyleukoemeraldine (LE) to polyemeraldine (EM) on the forward scan, and on the backward scan switching back to LE can be seen. The second peak at 0.68 V can be ascribed to the oxidation of head-to-tail dimmer. The third redox peak at about 0.98 V corresponds to the transition of EM to polypernigraniline (PE), while on the reversed scan the PE reduction to EM is also observed. [20]. From a comparison of PANI and PANI/SWNT, the polymerization behavior of the solution containing SWNT is similar in sharp to that from the single aniline solution, indicating that the mechanism of aniline polymerization is not significantly affected by the presence of SWNT. However, it should be noted that the current of peak C on the 30th cycle for PANI/SWNT is almost one order higher than that for pure PANI. This result reveals that the rate of aniline polymerization is undoubtedly enhanced by the presence of SWNT in the electrolytes. This may be because the SWNT are a good electron acceptor and aniline is a fairly good electron donor. The SWNT and aniline may form a charge-transfer couple in their ground state. Therefore, this couple with strong interactions leads to charge stabilization and thus effectively promotes the growth of PANI, and then they may serve as condensation nuclei to increase the propensity for the polymer to aggregate [21].

3.2. XPS analysis

To determine the structure and polymeric degree, the PANI and PANI/SWNT films were subjected to the XPS examination to investigate the effect of incorporated SWNT on intrinsic structure of polyaniline matrix. A typical XPS core-level N 1s for the PANI films and PANI/SWNT composite film are shown in Fig. 2. These core level spectra show relatively broad peaks, suggesting the existence of several structures. Thus, the XPS peaks of N 1s are reasonably composed of four Gaussian–Lorentzian peaks with the binding energy of 398.7, 400.0, 401.2, and 402.6 eV, respectively. The peak with the lowest binding energy (398.7 eV) is due to the neutral and imine-like (=N–) structure, and the peak centered at 400.0 eV is attributed to neutral and amine-like nitrogen atoms (–NH–) [22]. The peak centered at 401.2 eV is attributed to the nitrogen atom with a delocalized positive charge $N^{\bullet+}$ on the polymer backbone compensated with the counterions (SO_4^{2-}) and the highest binding energy (402.6 eV) peak is due to the protonated amine units. All these peaks are characteristic to the doped PANI. Especially, The ratio of [=N–]/[–NH–] can provide a direct evaluation of the intrinsic oxidation state of PANI and is indicative of the polymeric level in the polymer [23]. Therefore, the effect of SWNT on the intrinsic oxidation

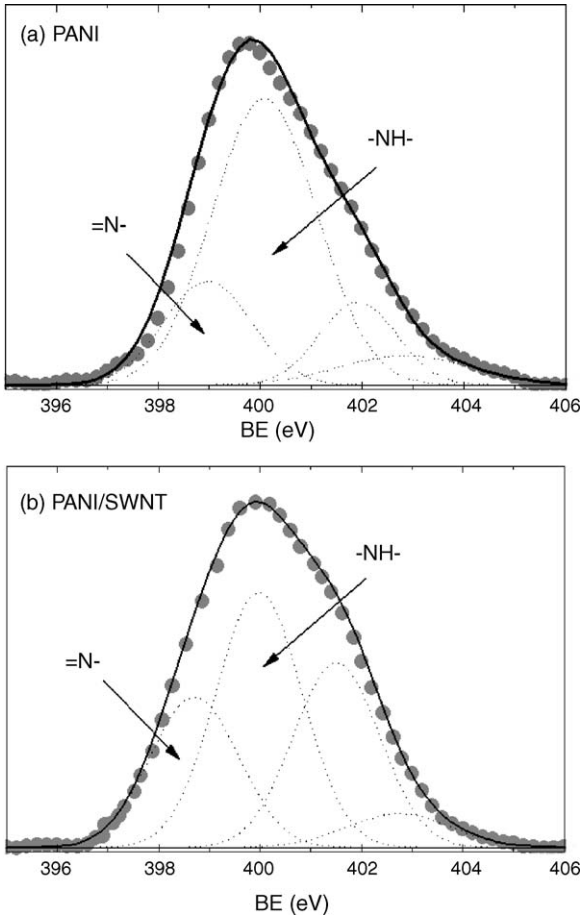

Fig. 2. XPS spectra of N 1s for (a) PANI and (b) PANI/SWNT film.

Table 1
Narrow scan XPS for PANI and PANI/SWNT films

Sample	Relative concentration (at.%)				N 1s (%)	C 1s(%)			
	C 1s	N 1s	O 1s	S 2p	[=N−]/[−NH−]	C−C/C−H	C=N	C=N$^+$/C−O	>C=O
PANI	58.6	9.7	27.9	3.8	0.30	40	28	18	14
PANI/SWNT	63.7	9.6	23.2	3.5	0.59	45	37	16	2

state and doping level of PANI can be quantitatively calculated from the [=N−]/[−NH−] ratio (Table 1) and the results exhibit that the intrinsic oxidation state of the PANI/SWNT is increased due to the incorporation of SWNT.

The XPS core level spectra of C 1s for the PANI and PANI/SWNT film are also shown in Fig. 3. All these C 1s spectra show the asymmetric characteristics, indicating the presence of structure defects [24]. Through Gaussian–Lorentzian fitting, these C 1s spectra can be fitted into four components at 284.7 (C–C or C–H), 285.9 (C=N), 286.6 (C=N$^+$ or –C–O) and 287.9 eV (>C=O), respectively [25]. The presence of carbonyl carbons >C=O appeared at highest binding energy is formed by the attack of water molecular during the polymerization [26]. The relative area of four peaks were calculated and also reported in Table 1. In particular, the relative area of these two higher binding-energy peaks (centered at 286.6 and 287.9 eV) is used to evaluate the density of carbonyl defects within polymers, showing the degradation of the polymer [27]. From the results of Table 1, comparing to pure PANI film, the defect density in PANI/SWNT composite film is decreased due to the incorporation of SWNT. As a result, the XPS analysis shows that the PANI film doped with SWNT has a higher polymeric degree and lower defect density, which probably results in better electrochemical properties and conductivity.

In addition, the PANI coverage in PANI/SWNT composite film can be estimated from relative amounts of carbon and nitrogen atoms at the surface [28]. As measured by XPS the (N/C) in single PANI is 0.165, which is very close to the theoretical value (0.167). In the case of PANI/SWNT, the (N/C) value is 0.150 and the calculated coverage of PANI is about 90.1% ($(N/C)_{PANI/SWNT}/(N/C)_{PANI}$) indicating the well incorporation of SWNT in PANI matrix.

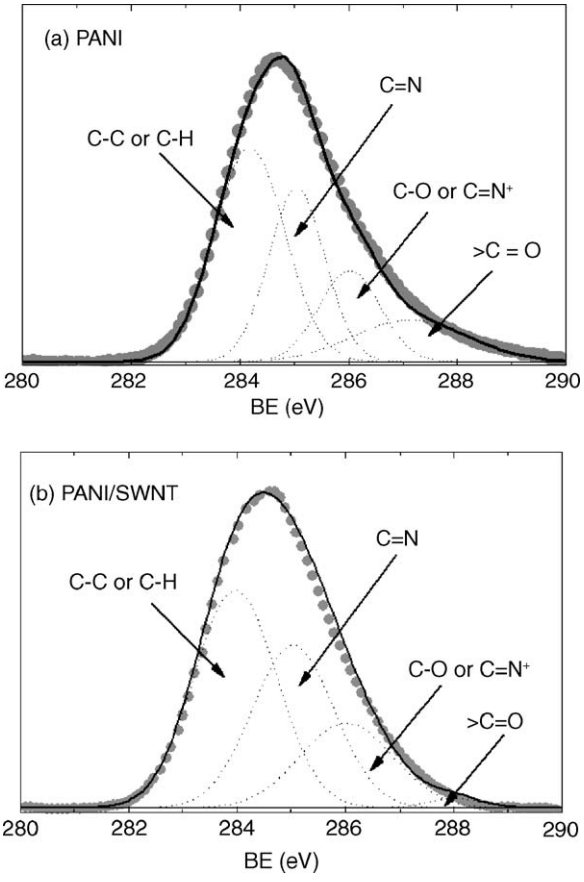

Fig. 3. XPS spectra of C 1s for (a) PANI and (b) PANI/SWNT film.

3.3. TEM of PANI and PANI/SWNT films

TEM of PANI and PANI/SWNT composite film are shown in Fig. 4. As shown in Fig. 4(a) and (b), PANI appears dendritic structure with the dimension range of 100–150 nm. Comparing with PANI, it was found that SWNT slight affected the sharp of resulting PANI/SWNT composite as shown in Fig. 4(c). However, it should be noticed that the edge of PANI is relatively smooth (Fig. 4(b)), while as for PANI/SWNT, SWNT obviously appears at the edge of the composite film exhibiting fine filar across the field of view for local magnified TEM images (Fig. 4(d)). Therefore, combination of XPS and TEM analyses seems to prove that the SWNT was incorporated into PANI matrix and only a fraction is bare.

3.4. Electrochemical characterization

The CV curves of PANI/SWNT and PANI films in 0.5 M H_2SO_4 solution are presented in Fig. 5. From CV curves, the currents at chosen potential (0.65 V) associated to double-layer capacitance can be obtained and are depended on the concentrations of the surface groups. The presence of surface functional groups can enhance hydrophilism and thereby facilitate the access of the electrolyte to the internal pore structure and increase the effective accessible surface area S_a ($m^2\ g^{-1}$) of the polymer films. Meanwhile, S_a is related to the gravimetric double-layer capacitance C ($F\ g^{-1}$) and may be calculated at a given scan rate v as $C = I/vm$ [29], where I is the current and m is the electrode mass. So the S_a can be estimated as specific value from the gravimetric capacitance C of

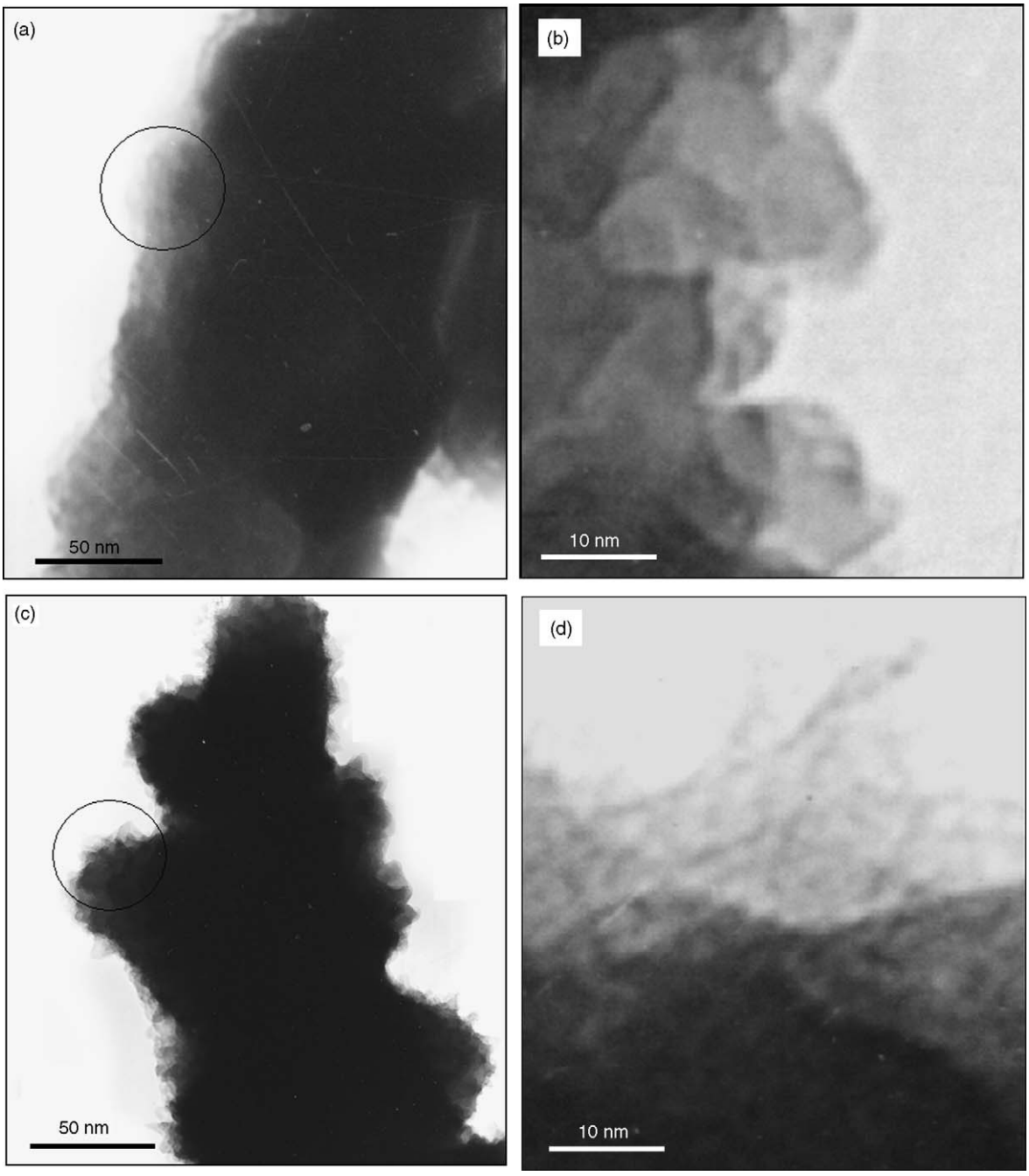

Fig. 4. TEM images of PANI (a and b) and PANI/SWNT (c and d) film.

polymer films by the equation $S_a = C/C_{GC}$, where C_{GC} is the double-layer capacitance ($F\,m^{-2}$) of glassy carbon electrode surface, for which the typical value of $0.2\,F\,m^{-2}$ was used. On the basis of the above equations, the S_a for PANI/SWNT composite film is $1026.2\,m^2\,g^{-1}$ and obviously higher than that of PANI ($257.5\,m^2\,g^{-1}$). Accordingly, the PANI/SWNT composite films, which have highly accessible surface area will have more active sites for electrochemical reaction than PANI film. Therefore, we can expect the SWNT have an obviously positive effect to PANI in term of their application in electrocatalysts.

Impedance spectra of the conducting polymer matrix may be considered to study the characteristics of film conductivity, structures and charge transport in polymer film/electrolyte interface. Therefore, the Nyquist plots for PANI and PANI/SWNT films after 30 cycle numbers of CV for electropolymerization are shown in Fig. 6(a) and (b), respectively. It can be seen that although the SWNT had been incorporated into polyaniline matrix, both of the impedance spectra of the films display similar characteristics, which the impedance spectra consist of a depressed semicircle at high frequencies followed by a linear spike at low frequencies.

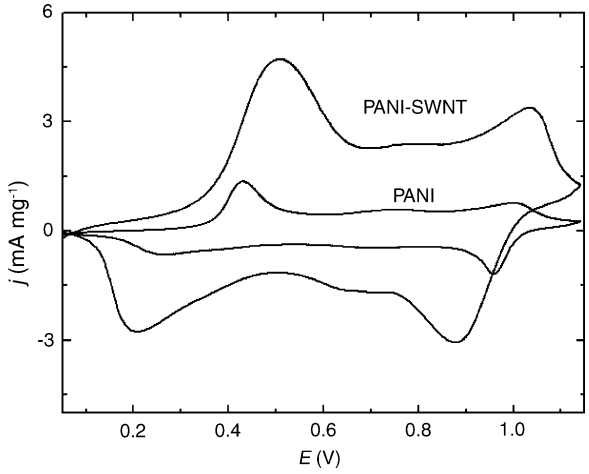

Fig. 5. Cyclic voltammograms of PANI and PANI/SWNT films in 0.5 M H_2SO_4 solution at a sweep rate of 20 mV s^{-1}.

Thus an equivalent circuit shown in Fig. 7 would be used to represent the impedance behavior of PANI and PANI/SWNT composite film in H_2SO_4 solution at open circuit potential. In this circuit, the high frequency intercept on real axis is due to solution resistance (R_{el}). A parallel combination of R_{ct} and Q_{dl} has been considered to form the semicircle, whose diameter has been considered as the charge-transfer resistance (R_{ct}) representing the rate of charge exchange between ions in aqueous and polymer chain at electrochemical interface. Considering the porous nature of PANI and PANI/SWNT films, double-layer capacitance was expressed as constant phase elements (CPE) Q_{dl} ($Z_{CPE} = A(j\omega)^{-n}$) in the equivalent-circuit models. The physical meaning of Q_{dl} and n are related to the accessible surface area of PANI and PANI/SWNT film in electrochemical reactions. Meanwhile, due to the semi-infinite diffusion of anions at the polymer–electrolyte interface, a straight line at low frequencies can be expressed by using a Warburg diffusion element (W) [30]. R_f and C_f represent electronic resistance and faradaic pseudo-capacitance of polymer film, respectively.

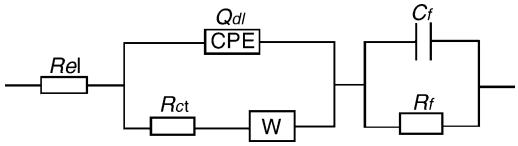

Fig. 7. Equivalent circuit for PANI and PANI/SWNT film in H_2SO_4 solution: R_{el}, solution resistance; R_{ct}, charge-transfer resistance; Q_{dl}, constant phase element related to double-layer capacitance; W, Warburg impedance; R_f, film resistance; C_f, film capacitance.

The corresponding solid lines in Fig. 6 are the fitted curves according to the equivalent circuit. The good fitting results implies that the equivalent circuit models can reasonably explain the electrochemical processes occurring in PANI and PANI/SWNT films at open circuit potential. According to the equivalent circuit, the simulated values of the impedance parameters were determined by CNLLS fitting procedure and listed in Table 2. By comparing fitted results between PANI films and PANI/SWNT composite films, greater Q_{dl} and smaller R_{ct} values were found for PANI/SWNT film, suggesting higher S_a and easier charger-transfer at interface (polymer/electrolyte). Increment of S_a of the composite film surface might be a part of reason causing increase in Q_{dl}. Another reasonable explanation for larger Q_{dl} maybe is due to better hydrophilic ability of PANI/SWNT composite film. Meanwhile, higher S_a and porous structure can also explain increasing W values representing promotion of mass diffusion.

Moreover, the film resistance R_f was also found to decrease from 10.2 Ω cm^2 for PANI to 2.5 Ω cm^2 for PANI/SWNT composite film and C_f from 3.9 to 2.2 μF cm^{-2} after 30 cycle electropolymerization, which is also attributed the enhancement of the electronic conductivity due to the interaction between PANI and SWNT increasing the effective degree of electron delocalization and the dopant effect or charge-transfer from the quinoid unit of PANI to the SWNT.

3.5. Morphology of Pt-PANI and Pt-PANI/SWNT

To investigate the morphology of Pt particles into PANI and PANI/SWNT films and its influence on methanol oxida-

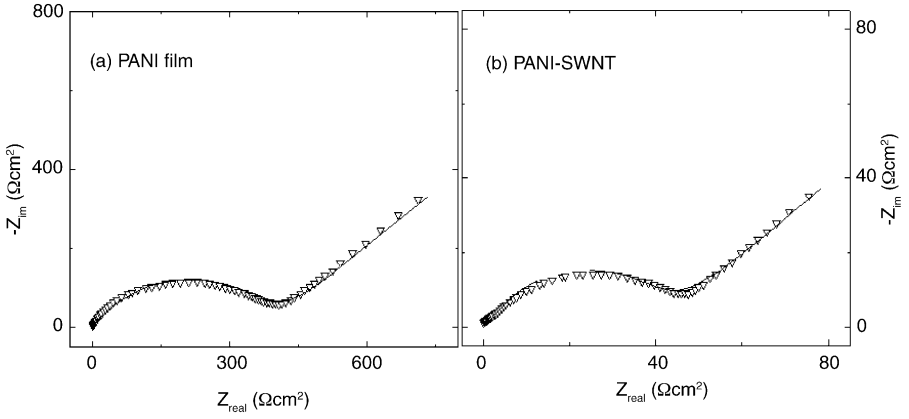

Fig. 6. Nyquist plots of PANI (a) and PANI/SWNT (b), solid line is fitted results.

Table 2
Fitted parameters of the elements on equivalent circuits for PANI and PANI/SWNT films in 0.5 M H_2SO_4 solution at open circuit potential

Films	CPE ($\times 10^5\ \Omega^{-1}\ s^n\ cm^{-2}$)	n	R_{ct} ($\Omega\ cm^2$)	W ($\times 10^3\ \Omega^{-1}\ cm^{-2}\ s^{0.5}$)	C_f ($\times 10^6\ F\ cm^{-2}$)	R_f ($\Omega\ cm^2$)
PANI	3.2	0.71	375	3.1	3.9	10.2
PANI/SWNT	12.1	0.69	45	6.8	2.2	2.5

tion, SEM and TEM images of Pt-PANI and Pt-PANI/SWNT are shown in Figs. 8 and 9, respectively.

It can be seen from SEM observation for both Pt-PANI and Pt-PANI/SWNT, the particles are spread in a homogeneous arrangement on polymer matrix. However, it was found that the incorporation of SWNT strongly affected the morphology of Pt particles deposited on polymer films at the same conditions. Moreover, the Pt-PANI/SWNT shows a loose and well-distributed structure, which exhibits a fine Pt particles varying size between 10 and 80 nm. In the case of Pt-PANI, the Pt particle exhibit coarse granules with a size ranges from 50 to 120 nm.

In addition, despite SWNT cannot clearly observe at this magnification for SEM, according to previous XPS and TEM analyses, the SWNT had been well incorporated into PANI matrix.

Fig. 9 shows the TEM images of Pt particles deposited on PANI and PANI/SWNT composite films. The large gray parts are the images of PANI and PANI/SWNT, while the scattered black spots are the images of Pt particles. The averaged size and distribution of Pt particles were obtained by randomly measuring the sizes of at least 100 particles in the magnified images. The TEM observation is well agreed with that of SEM, which averaged size of Pt particle deposited on PANI/SWNT is approximate 20 nm and obviously smaller than that of Pt on PANI film (about 80 nm).

These results may reveal Pt-PANI/SWNT has considerably higher dispersion and utilizations of Pt than those of

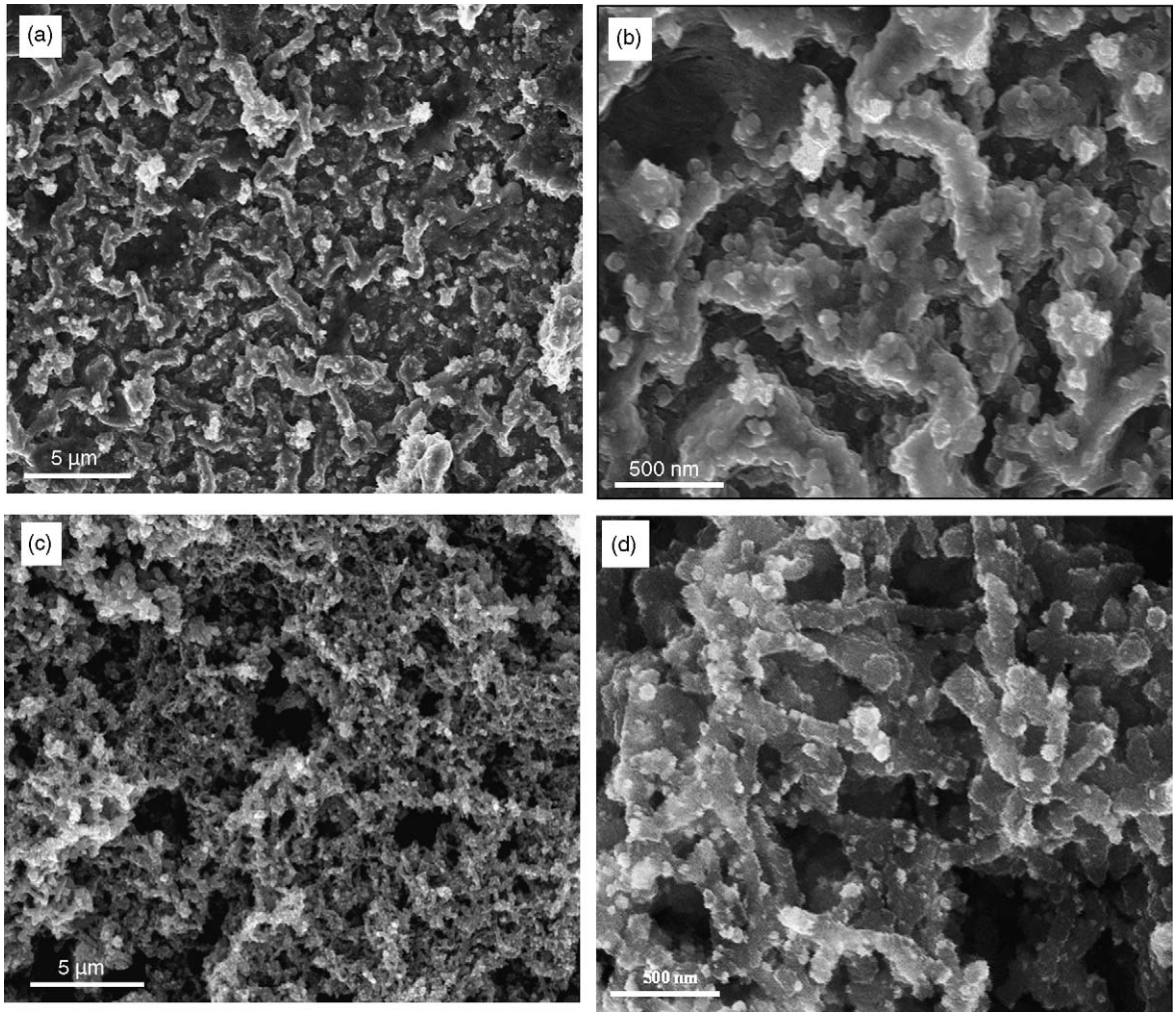

Fig. 8. SEM images of Pt-PANI (a and b) and Pt-PANI/SWNT (c and d) at Pt loading of 80 μg cm^{-1}.

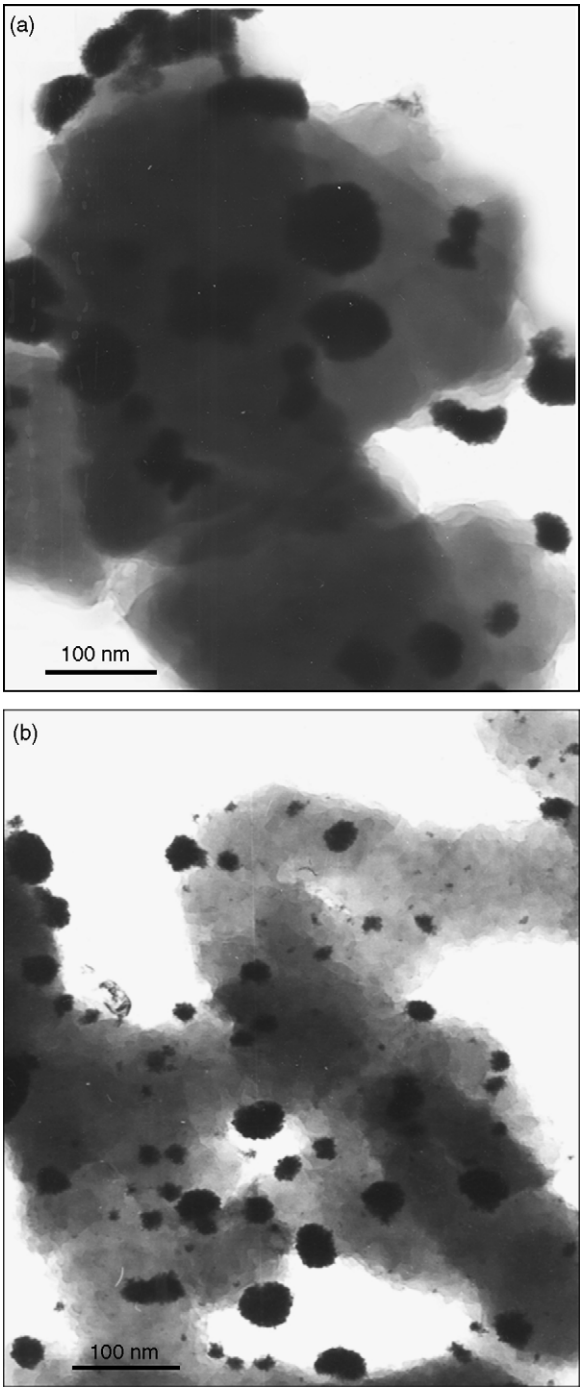

Fig. 9. TEM images of Pt-PANI (a) and Pt-PANI/SWNT (b), at Pt loading of 80 μg cm^{-1}.

Pt-PANI, which can be attributed to the larger accessible surface area and faster charge-transfer of the composite films according to electrochemical characteristics (CV, EIS) of PANI/SWNT.

3.6. Methanol electrooxidation

To evaluate the effect of incorporation of SWNT into PANI matrix on methanol electrooxidation, the variation in current densities of methanol oxidation representing mass activity with Pt loadings on Pt-PANI and Pt-PANI/SWNT electrodes was shown in Fig. 10. It is evident that for Pt-PANI/SWNT, as the Pt loading increases, there is a continuous increase in activity from 6.1 mA cm^{-2} (Pt = 30 μg cm^{-2}) to 10.1 mA cm^{-2} (Pt = 140 μg cm^{-2}). These data also indicate that the current increases nearly linearly with increased Pt loadings, supporting that increased Pt deposition results in an increase in the number of Pt particles and not an increase in size of the particles. In the case of Pt-PANI catalyst, the activity was increased from 1.3 (Pt = 30 μg cm^{-2}) to 3.0 mA cm^{-2} (Pt = 100 μg cm^{-2}). Beyond this loading, the activity saturates at approximate 3.1 mA cm^{-2}. This reflects that the composite polymer structure helps to achieve a fine dispersion of Pt particles inside the PANI/SWNT matrix. Therefore, comparing to PANI, the PANI/SWNT not only showed higher mass activity but also accommodated more Pt particles.

According to the previous results from CV, EIS characterization as well as morphology analysis (SEM, TEM), it can be concluded that the better Pt dispersion and utilization on PANI/SWNT is a main reason to enhance methanol electrooxidation on Pt-PANI/SWNT electrocatalyst. In addition, high conductivity (ionic and electronic) of PANI/SWNT composite film also contributes to achieve high current density of methanol oxidation. Fig. 11 shows typical current–time responses for methanol oxidation at 0.65 V on Pt-PANI and Pt-PANI/SWNT catalysts in 0.5 M CH_3OH + 0.5 M H_2SO_4. As expected, the methanol oxidation current at Pt-PANI/SWNT is obviously higher than that of Pt-PANI. In addition, it should be noticed that both Pt-PANI and Pt-PANI/SWNT catalysts present a current decay in current–time measurements, which was also observed for traditional Pt [31] and PtRu catalysts [32] attributing to the formation of some Pt oxide or adsorbed intermediates in methanol electrooxidation reaction [33]. However, the most

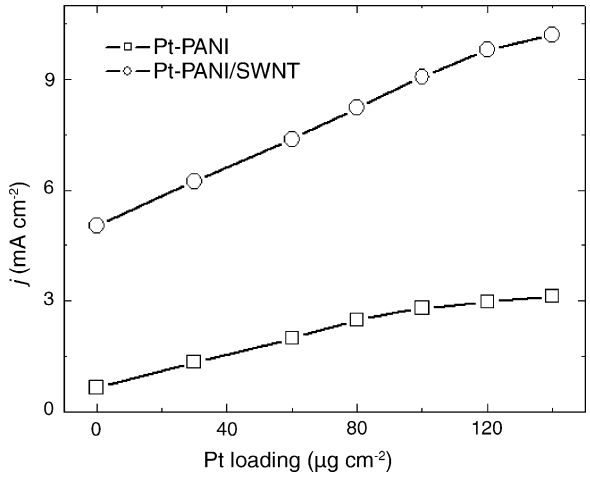

Fig. 10. Current density of methanol electrooxidation at 0.65 V with various Pt loading. Current density were measured at 0.65 V from CV in 0.5 M CH_3OH + 0.5 M H_2SO_4 at a sweep rate of 20 mV s^{-1}.

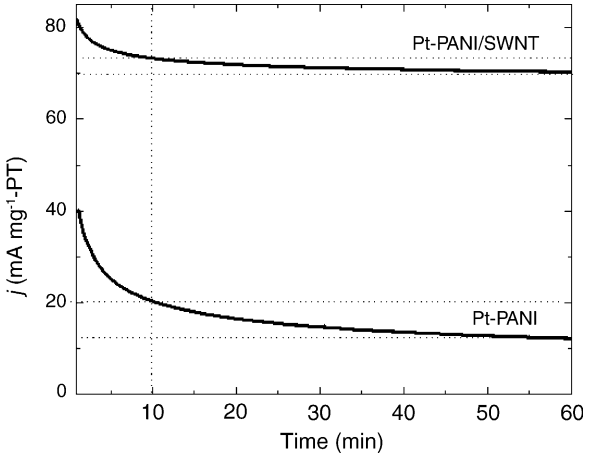

Fig. 11. Current–time curves of methanol electrooxidation in 0.5 M CH_3OH + 0.5 M H_2SO_4 on Pt-PANI and Pt-PANI/SWNT with Pt loading of 80 μg cm^{-2} at 0.65 V.

interesting feature deserving our attention is that the decrease in current density was found to be around 4.0% for the Pt-PANI/SWNT from 10 to 60 min and the corresponding decrease for Pt-PANI was found to be 41.8%. This demonstrates that the activity and the stability of the Pt incorporated PANI/SWNT composite film was higher than the Pt deposited into single PANI film.

4. Conclusion

In this work, we demonstrate the incorporation of SWNT into the PANI matrix during electropolymerization process by electrochemical codeposition technique. The incorporation of SWNT into PANI matrix not only leads to significant improvement for higher oxidation degree and lower defect density in PANI structure but also causes higher accessible surface areas, electronic conductivity and easier charge-transfer between polymer/electrolyte interfaces. Moreover, our results show that Pt deposited on PANI/SWNT composite support has considerably higher dispersion and utilizations of Pt than that on PANI film and can be used as an electrocatalyst for methanol oxidation with high performance and stability. In addition, the catalysts can also be employed for hydrogen and other low-molecular alcohol in proton exchange membrane (PEM) fuel cells. It should be stressed that in Pt-PANI/SWNT catalyst, the electrocatalytic properties can also be affected by amounts of SWNT incorporated into PANI and the morphology of electrodeposited Pt particles associated with the conditions in polymerization and electrodeposition process, which is currently under our investigation.

We believe that the combination of PANI/SWNT composite materials with large electrochemical accessible surface area, well conductive polymer and a metal with catalytic properties will yield a very effective electrochemical catalyst.

Acknowledgements

The authors wish to acknowledge the financial support of this work from Ministry of Science and Technology (Grant: G2000026408), NSF (Grant: 20125310) and Postdoctoral Science Foundation (2004035300) of China. We also wish to thank Prof. Yongsheng Chen in Nankai University for his friendly supply of SWNT samples.

References

[1] R. Dillon, S. Srinivasan, A.S. Arico, V. Antonucci, J. Power Sources 127 (2004) 112–126.
[2] A.S. Arico, V. Baglio, E. Modica, A. Blasi, V. Antonucci, Electrochem. Commun. 6 (2004) 164–169.
[3] M. Carmo, V.A. Paganin, J.M. Rosolen, E.R. Gonzalez, J. Power Sources 142 (2005) 169–176.
[4] C.A. Bessel, K. Laubernds, N.M. Rodriguez, R.T.K. Baker, J. Phys. Chem. B 105 (2001) 1115–1118.
[5] E.S. Steigerwalt, G.A. Deluga, D.E. Cliffel, C.M. Lukehart, J. Phys. Chem. B 105 (2001) 8097–8101.
[6] Z.L. Liu, X.H. Lin, J.Y. Lee, W. Zhang, M. Han, L.M. Gan, Langmuir 18 (2002) 4054–4060.
[7] W.Z. Li, C.H. Liang, W.J. Zhou, J.S. Qiu, Z.H. Zhou, G.Q. Sun, Q. Xin, J. Phys. Chem. B 107 (2003) 6292–6299.
[8] J.E. Huang, D.J. Guo, Y.G. Yao, H.L. Li, J. Electroanal. Chem. 577 (2005) 93–97.
[9] Y.C. Liu, X.P. Qiu, Y.Q. Huang, W.T. Zhu, Carbon 40 (2002) 2375–2380.
[10] Y.C. Liu, X.P. Qiu, Y.Q. Huang, W.T. Zhu, G.S. Wu, J. Power Sources 114 (2003) 10–14.
[11] B. Philip, J.N. Xie, J.K. Abraham, V.K. Varadan, Polym. Bull. 53 (2005) 127–138.
[12] R. Sainz, A.M. Benito, M.T. Martinez, J.F. Galindo, J. Sotres, A.M. Baro, B. Corraze, O. Chauvet, W.K. Maser, Adv. Mater. 17 (2005) 278–282.
[13] T.M. Wu, Y.W. Lin, C.S. Liao, Carbon 43 (2005) 734–740.
[14] G.B. Blanchet, C.R. Fincher, F. Gao, Appl. Phys. Lett. 82 (2003) 1290–1292.
[15] I. Becerik, F. Kadirgan, J. Electrochem. Soc. 148 (2001) D49–D54.
[16] M.J. Croissant, T. Napporn, J.M. Leger, C. Lamy, Electrochim. Acta 43 (1998) 2447–2457.
[17] G.M.D. Nascimento, P. Corio, R.W. Novickis, M.L.A. Temperini, M.S. Dresselhaus, J. Polym. Sci., Part A: Polym. Chem. 43 (2005) 815–822.
[18] J. Chen, M.A. Hamon, H. Hu, Y.S. Chen, A.M. Rao, P.C. Eklund, R.C. Haddon, Science 282 (1998) 95–98.
[19] D.E. Stilwell, S.M. Park, J. Electrochem. Soc. 135 (1988) 2491–2496.
[20] M. Barth, M. Lapkowski, S. Lefrant, Electrochim. Acta 44 (1999) 2117–2123.
[21] Y. Sun, S.R. Wilson, D.I. Schuster, J. Am. Chem. Soc. 123 (2001) 5348–5349.
[22] N.K. Svelko, S. Reynaud, R. Dedryvere, H. Martinez, D. Gonbeau, J. Francois, Langmuir 21 (2005) 1575–1583.
[23] Y.K. Zhou, B.L. He, W.J. Zhou, H.L. Li, J. Electrochem. Soc. 151 (2004) A1052–A1057.
[24] E.T. Kang, K.G. Neoh, K.L. Tan, Handbook of Organic Conductive Molecules and Polymers, Wiley, New York, 1997, pp. 180–213.
[25] G. Beamson, D. Briggs, High Resolution XPS of Organic Polymer, the Scienta ESCA300 Database, Wiley, New York, 1992, pp. 56–79.
[26] F. Beck, Electrochim. Acta 33 (1988) 839–843.
[27] P. Schottland, K. Zong, C.L. Gaupp, B.C. Thompson, C.A. Thomas, I. Giurgiu, R. Hickman, K.A. Abboud, J.R. Reynolds, Macromolecules 33 (2000) 7051–7061.

[28] M.P. Seah, W.A. Dench, Surf. Interf. Anal. 1 (1979) 2–6.
[29] Y.K. Zhou, B.L. He, W.J. Zhou, J. Huang, X.H. Li, B. Wu, H.L. Li, Electrochim. Acta 49 (2004) 257–262.
[30] A. Tarola, D. Dini, E. Salatelli, F. Andreani, F. Decker, Electrochim. Acta 44 (1999) 4189–4193.
[31] A.P. O'Mullane, S.E. Dale, J.V. Macpherson, P.R. Unwin, Chem. Commun. 4 (2004) 1606–1607.
[32] G. Wu, L. Li, B.Q. Xu, Electrochim. Acta 50 (2004) 1–10.
[33] H. Hoster, T. Iwasita, H. Baumgartner, W. Vielstich, J. Electrochem. Soc. 148 (2001) A496–A501.